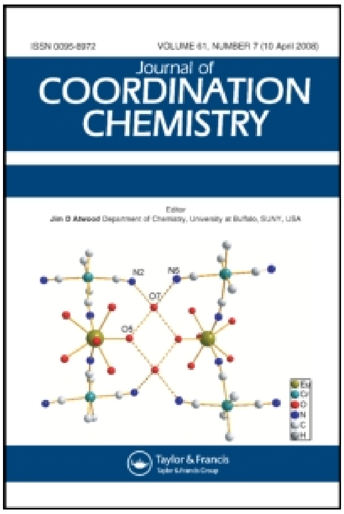

Journal of Coordination Chemistry
Publication details, including instructions for authors and subscription information:
http://www.informaworld.com/smpp/title~content=t713455674

Three-dimensional 3d-4f hetero-bimetallic coordination polymers through hydrogen bonds: synthesis, structures and mössbauer spectrum analysis

Guangming Li[ab]; Takashiro Akitsu[a]; Osamu Sato[c]; Yasuaki Einaga[a]
[a] Department of Chemistry, Keio University, 3-14-1 Hiyoshi, Yokohama 223-8522, Japan [b] Faculty of Chemistry and Chemical Engineering, Heilongjiang University, Harbin 150080, P.R. China [c] Special Research Laboratory for Optical Science, Kanagawa Academy of Science and Technology, 3-2-1 Sakado, Kawasaki 213-0012, Japan

To cite this Article Li, Guangming , Akitsu, Takashiro , Sato, Osamu and Einaga, Yasuaki(2004) 'Three-dimensional 3d-4f hetero-bimetallic coordination polymers through hydrogen bonds: synthesis, structures and mössbauer spectrum analysis', Journal of Coordination Chemistry, 57: 10, 855 — 864

To link to this Article: DOI: 10.1080/00958970410001721439

URL: http://dx.doi.org/10.1080/00958970410001721439

J. Coord. Chem., Vol. 57, No. 10, 10 July 2004, pp. 855–864

Taylor & Francis
Taylor & Francis Group

THREE-DIMENSIONAL 3d–4f HETERO-BIMETALLIC COORDINATION POLYMERS THROUGH HYDROGEN BONDS: SYNTHESIS, STRUCTURES AND MÖSSBAUER SPECTRUM ANALYSIS

GUANGMING LI[a,c], TAKASHIRO AKITSU[a],
OSAMU SATO[b] and YASUAKI EINAGA[a,*]

[a]*Department of Chemistry, Keio University, 3-14-1 Hiyoshi, Yokohama 223-8522, Japan;*
[b]*Special Research Laboratory for Optical Science, Kanagawa Academy of Science and Technology, KSP Building East 412, 3-2-1 Sakado, Kawasaki 213-0012, Japan;*
[c]*Faculty of Chemistry and Chemical Engineering, Heilongjiang University, Harbin 150080, P.R. China*

(Received 21 July 2003; Revised 20 October 2003; In final form 18 April 2004)

Four cyano-bridged 3d–4f hetero-bimetallic Ln(III)–Fe(III) assemblies, $\{[Ln(DMF)_4(H_2O)_3(\mu\text{-}CN)Fe(CN)_5]\cdot H_2O\}_n$ (Ln = Ce (**1**), Nd (**2**), Sm (**3**) and Gd (**4**); DMF = *N*,*N*-dimethylformamide), have been synthesized. X-ray crystallographic analysis of both **3** and **4** reveals three-dimensional network structures resulting from hydrogen bonds in the crystals. With respect to the coordination number on Sm(III) atoms, **3** is different from previously reported structures. Structural comparison indicates that the differences in magnetic properties between **3** and **4** do not derive from structural factors. Mössbauer spectra at both 298 and 10 K reveal that the characteristic quadrupole splitting for low-spin Fe(III) ions ($S = 1/2$) remains unchanged, indicating that the spin state of Fe(III) ions in **1**–**4** is not affected by temperature. The magnetic anisotropy derived from the ground states of Ln(III) ions with odd $4f^n$ electrons ($n = 1$, 3, 5 and 7), $^2F_{5/2}$, $^4I_{9/2}$, $^6H_{5/2}$ and $^8S_{7/2}$ for Ce(III), Nd(III), Sm(III) and Gd(III), respectively, dominates the exchange interaction in the Ln(III)–NC–Fe(III) systems.

Keywords: Synthesis; Crystal structures; Mössbauer spectra; 3d–4f complex; Cyano-bridged

INTRODUCTION

Investigations of the synthesis and magnetic properties of cyano-bridged 3d–4f hetero-bimetallic assemblies have been driven by interest in novel molecule-based magnets, such as $Ln(phen)_2(H_2O)_2Fe(CN)_6$ (phen = 1,10-phenanthroline) [1], $Ln(DMA)_2(H_2O)_4Fe(CN)_6\cdot 6H_2O$ (DMA = *N*,*N*-dimethylacetamide) [2], $[Ln(C_4H_7ON)_2(H_2O)_3Fe(CN)_6]\cdot 2H_2O$ [3] and $Ln(DMF)_4(H_2O)_3Fe(CN)_6\cdot H_2O$ (DMF = *N*,*N*-dimethylformamide) [4–7]. Various magnetic properties of 3d–4f bimetallic assemblies derive from

---

*Corresponding author. Fax: +81-45-566-1697. E-mail: einaga@chem.keio.ac.jp

ISSN 0095-8972 print: ISSN 1029-0389 online
DOI: 10.1080/00958970410001721439

the spin and orbital angular momentum of Ln(III) ions. Furthermore, the electronic configuration of Ln(III) ions may be split into ${}^{2s+1}L_J$ states by interelectronic repulsion, spin–orbit coupling and Stark components. Many different magnetic interactions of the 3d–4f systems have been reported previously, including antiferromagnetic interactions for Ln = La–Eu ($4f^n$ where $n < 7$) and ferromagnetic interactions for Ln = Gd ($4f^7$ and $L = 0$) and Ln = Tb–Yb ($4f^n$ where $n > 7$) [20]. By contrast, magnetic interactions of a series of $[Ln(DMF)_4(H_2O)_3(\mu\text{-}CN)Fe(CN)_5]\cdot H_2O$ complexes were antiferromagnetic for Ln = Ce, Nd, Gd and Dy, ferromagnetic for Ln = Tb, Ho and Tm, and had no significant interaction for Ln = Pr, Eu, Er, Sm and Yb [7]. However, magnetic interaction between 3d and 4f metal ions is generally difficult to interpret. Necessary theoretical models for simple dinuclear compounds need to be developed. Because the type of exchange interaction depends not only on orbital contributions of the Ln(III) ions but also on the magnetic anisotropy of the Fe(III) ions, the spin states of the Fe(III) ions should be identified separately. In addition, it is proposed that appropriate arrangement of bridged-metal ions is important for magnetic interaction [8]. In this article, we explore the correlations among magnetic interactions, structures and spin states of Fe(III) ions. Therefore, the structural parameters for **3** and **4**, which showed significant differences with respect to magnetic properties, have been compared in detail. The spin states of Fe(III) ions have been studied by Mössbauer spectra at both 298 and 10 K.

EXPERIMENTAL

General Procedures

All commercial-grade chemicals and solvents were used as purchased. Elemental analyses were carried out on an Elementar Vario EL at the Central Facilities for Science and Technology Research, Keio University. IR spectra (KBr disks) were recorded on a BIO-RAD FTS-165 FTIR spectrometer at 25°C over the range 400–4000 cm^{-1}. Mössbauer spectra were recorded by using a Topologic systems model 222 constant-acceleration spectrometer, with a ${}^{57}Co/Rh$ source, in the transmission mode. The temperature was controlled and monitored by a thermocouple together with the variable-temperature cryostat.

Synthesis

The synthesis followed a modified literature method [4,5]. Compounds **1**–**4** were obtained by carefully layering a DMF solution (10 mL) of $LnCl_3\cdot 6H_2O$ (1.0 mmol) on top of an equivalent aqueous solution (10 mL) of $K_3[Fe(CN)_6]$ (1.0 mmol) in a glass test-tube (30 mL) of diameter 15 mm. Large needle-shaped or small prismatic crystals were harvested at the interface of the two solutions after setting it aside for several days at room temperature (25°C). The crystalline compounds were collected by filtration.

$[Ce(DMF)_4(H_2O)_3(\mu\text{-}CN)Fe(CN)_5]\cdot H_2O$ (1)

Orange–yellow crystals. Yield: 90%. Anal. Calcd. for $C_{18}H_{36}CeFeN_{10}O_8$(%): C, 30.17; H, 5.06; N, 19.55. Found: C, 30.06; H, 5.03; N, 19.60. IR (cm^{-1}, KBr disk): ν_{OH}(ν-OH hydrogen bonding) 3405, ν_{CH}(CH stretching in ν-CH_3) 2938, ν_{CN}(ν-CN) 2143, 2125, 2061 and 2024, ν_{OH}(δ-HOH) 1648, ν_{CH}(C–H stretching in δ_{as}-CH_3) 1440, ν_{CH}(CH stretching in δ_s-CH_3) 1382, ν_{CN}(CN stretching) 1061.

$[Nd(DMF)_4(H_2O)_3(\mu\text{-}CN)Fe(CN)_5]\cdot H_2O$ (2)

Yellow crystals. Yield: 87%. Anal. Calcd. for $C_{18}H_{36}FeN_{10}NdO_8$(%): C, 30.00; H, 5.04; N, 19.44. Found: C, 30.05; H, 5.00; N, 19.83. IR (cm^{-1}, KBr disk): ν_{OH}(ν-OH hydrogen bonding) 3392, ν_{CH}(CH stretching in ν-CH_3) 2943, ν_{CN}(ν-CN) 2146, 2125, 2067 and 2024, ν_{OH}(δ-HOH) 1650, ν_{CH}(C–H stretching in δ_{as}-CH_3) 1439, ν_{CH}(CH stretching in δ_s-CH_3) 1382, ν_{CN}(CN stretching) 1059.

$[Sm(DMF)_4(H_2O)_3(\mu\text{-}CN)Fe(CN)_5]\cdot H_2O$ (3)

Yellow crystals. Yield: 90%. Anal. Calcd. for $C_{18}H_{36}FeN_{10}O_8Sm$(%): C, 29.75; H, 4.99; N, 19.27. Found: C, 29.59; H, 4.94; N, 19.22. IR (cm^{-1}, KBr disk): ν_{OH}(ν-OH hydrogen bonding) 3385, ν_{CH}(CH stretching in ν-CH_3) 2944, ν_{CN}(ν-CN) 2148, 2123, 2072 and 2024, ν_{OH}(δ-HOH) 1649, ν_{CH}(C–H stretching in δ_{as}-CH_3) 1438, ν_{CH}(CH stretching in δ_s-CH_3) 1381, ν_{CN}(CN stretching) 1059.

$[Gd(DMF)_4(H_2O)_3(\mu\text{-}CN)Fe(CN)_5]\cdot H_2O$ (4)

Yellow crystals. Yield: 90%. Anal. Calcd. for $C_{18}H_{36}FeGdN_{10}O_8$(%): C, 29.47; H, 4.95; N, 19.09. Found: C, 29.34; H, 4.91; N, 19.03. IR (cm^{-1}, KBr disk): ν_{OH}(ν-OH hydrogen bonding) 3373, ν_{CH}(CH stretching in ν-CH_3) 2939, ν_{CN}(ν-CN) 2151, 2124, 2077 and 2024, ν_{OH}(δ-HOH) 1653, ν_{CH}(C–H stretching in δ_{as}-CH_3) 1438, ν_{CH}(CH stretching in δ_s-CH_3) 1382, ν_{CN}(CN stretching) 1059.

X-ray Crystallography

Single crystals of **3** and **4** were coated and glued on the top of a glass fiber with epoxy resin. Intensity data were collected on a Rigaku AFC-7R four-circle diffractometer with graphite-monochromated Mo-Kα radiation ($\lambda = 0.71073$ Å) at 24°C. Although the decay was significant (19.99% for **3** and 2.16% for **4**) in the intensity of three standard reflections throughout the data collection, the corrections for decay were applied properly. The transmission factors for **3** and **4** were 0.8443–0.9998 and 0.9155–0.9996, respectively. All calculations were carried out with a teXsan program package [9] on an SGI O2 workstation. The structures were solved by direct methods using SIR92 [10] and refined on F^2 anisotropically for all nonhydrogen atoms by full-matrix least-squares methods with SHELXL-97 [11]. The hydrogen atoms of the DMF ligands were added to the geometrically calculated positions of C–H = 0.96 Å and were refined isotropically as riding models. However, the hydrogen atoms of the water molecules could not be included in the models. In fact, the residual electron density was found in some areas of the different Fourier maps. The maximum and minimum peaks were 2.42 and $-2.29\,e\,Å^{-3}$ for **3** and 6.87 and $-3.44\,e\,Å^{-3}$ for **4**, respectively.

RESULTS AND DISCUSSION

Crystal Structures

X-ray crystallographic analysis shows that **3** and **4** are isomorphous crystal structures, crystallizing in monoclinic, space group $P2_1/n$, and $Z = \mathbf{4}$ (Table I), in accordance with their Fe(III) and Co(III) analogs [7,12]. The Ln(III) ions have an eight-coordinated distorted square antiprism coordination geometry (approximately D_{4d} symmetry) with four DMFs, three waters and a cyano-bridged $[Fe^{III}(CN)_6]^{3-}$ moiety (Fig. 1). A nine-coordinate Sm(III) ion was reported in a closely related compound $[Sm(DMF)_4(H_2O)_4(\mu\text{-}CN)Fe(CN)_5] \cdot H_2O$ [6]. In fact, one bond distance (Sm–O = 2.885(5) Å) for this compound was considered too long to be regarded as a common coordination bond. In principal, Ln(III) ions can adopt various coordination numbers in the range 6 to 12. The large ions (La–Nd) generally have a nine-coordinate tricapped, trigonal-prismatic geometry, while small ions (Tb–Lu) afford an eight-coordinate square-antiprismatic geometry. The intermediate ions (Pm–Gd) are between the two coordination geometries [13]. The top square (Fig. 2) for **3** and **4** consists of the atoms of O(3), O(5), O(6) and O(7), coplanar with mean deviations of 0.010 and 0.023 Å, while the bottom one, O(1), O(2), O(4) and N(7), shares another plane with mean deviations of 0.193 and 0.187 Å. The dihedral angles between the two mean planes are 3.061 and 2.546° for **3** and **4**, respectively. The average bond distances for Ln(1)–O(1–4) (DMF) are 2.393 and 2.373 Å (see Table II), and for Ln(1)–O(5–7) (water) are 2.435 and 2.410 Å for **3** and **4**, respectively. Obviously, the former was slightly longer than the latter due to steric effects although the sum of ion radii of Ln(III) and O atoms should be identical (approximately 2.5 Å) [14,15].

TABLE I Crystallographic data for **3** and **4**

	3	**4**
Formula	$C_{18}H_{36}FeN_{10}O_8Sm$	$C_{18}H_{36}GdFeN_{10}O_8$
Formula weight	726.79	733.64
Crystal size/mm	0.50 × 0.30 × 0.30	0.50 × 0.30 × 0.30
Crystal system	Monoclinic	Monoclinic
Space group	$P2_1/n$ (No. 14)	$P2_1/n$ (No. 14)
a/Å	19.881(5)	19.806(7)
b/Å	8.885(8)	8.875(3)
c/Å	17.634(7)	17.633(6)
β/°	96.04(3)	96.25(3)
V/Å^3	3097(3)	3081(1)
Z	4	4
D_c/Mg m^{-3}	1.558	1.581
$F(000)$	1464	1472
$2\theta_{max}$/°	55.0	55.0
μ/mm^{-1} (Mo Kα)	2.402	2.662
No. of reflections observed ($I > 2\sigma(I)$)	8504	8294
No. of unique reflections (R_{int})	7134 (0.107)	7088 (0.027)
No. of reflections used	5714	5389
No. of parameters	344	344
R_1[a]	0.052	0.067
R_w[b]	0.153	0.269
Goodness-of-fit	1.05	1.05

[a] $R_1 = \Sigma||F_o| - |F_c||/\Sigma|F_o|$ for the data $I > 2\sigma(I)$.

[b] $R_w = (\Sigma w|F_o| - |F_c|)^2/\Sigma(w|F_o|^2))^{1/2}$ for all data, $w = [\sigma^2(F_o)^2 + (0.1101P)^2 + 3.6801P]^{-1}$ for **3** and $w = [\sigma^2(F_o)^2 + (0.0986P)^2 + 166.6037P]^{-1}$ for **4**, where $P = (F_o^2 + 2F_c^2)/3$.

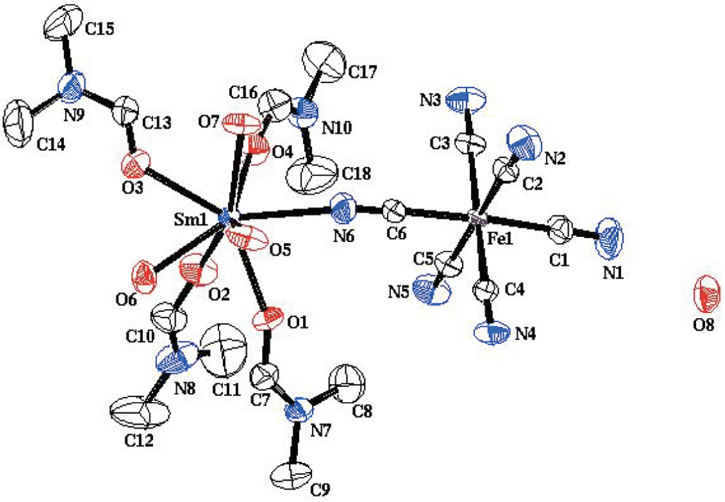

FIGURE 1 A view of the molecular structure of **3**. Hydrogen atoms are omitted for clarity.

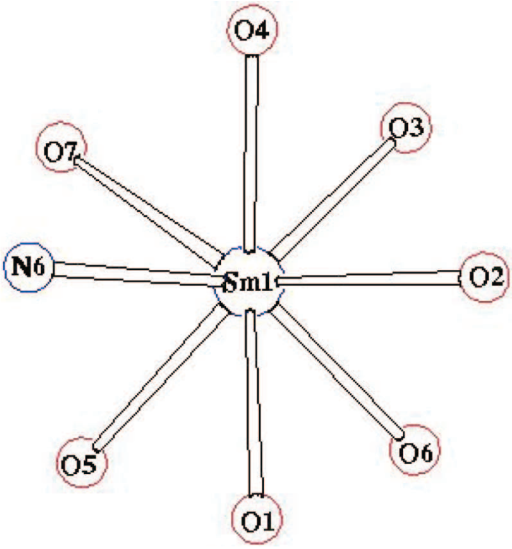

FIGURE 2 Coordination sphere of the eight-coordinate anti-prism geometry around Sm(III) for **3**.

The Fe(III) ions have a six-coordinate, distorted octahedral geometry (approximately O_h symmetry) coordinated by six cyanide ligands. The average bond distances for Fe(1)–C(1–6) and C(1–6)–N(1–6) are 1.94 and 1.16 Å, respectively. These bond distances are the same as the corresponding values of 1.94 and 1.16 Å for $[Fe^{III}(CN)_6]^{3-}$ of the analogous bimetallic complexes in the CSD [16]. All of the *trans*-C–Fe–C bond angles are close to 180°; however, some bond angles of C–Fe–C, such as C(2)–Fe(1)–C(4) = 88.7(2) and 87.8(6)°, C(2)–Fe(1)–C(6) = 91.5(2) and 91.8(5)° and C(4)–Fe(1)–C(5) = 92.5(2) and 93.0(6)° for **3** and **4**, respectively, deviate significantly from 90°. As for the cyanide bridge, the bond angles of Ln(1)–N(6)–C(6) are

TABLE II Selected bond distances (Å) and bond angles (°) for **3** and **4**

	3	**4**
Ln(1)–O(1)	2.381(5)	2.36(1)
Ln(1)–O(2)	2.414(5)	2.39(1)
Ln(1)–O(3)	2.407(4)	2.39(1)
Ln(1)–O(4)	2.369(5)	2.35(1)
Ln(1)–O(5)	2.444(5)	2.42(1)
Ln(1)–O(6)	2.434(4)	2.41(1)
Ln(1)–O(7)	2.428(4)	2.40(1)
Ln(1)–N(6)	2.505(5)	2.51(1)
Fe(1)–C(1)	1.933(6)	1.93(1)
Fe(1)–C(2)	1.931(5)	1.92(1)
Fe(1)–C(3)	1.937(6)	1.94(1)
Fe(1)–C(4)	1.941(6)	1.94(1)
Fe(1)–C(5)	1.947(5)	1.95(1)
Fe(1)–C(6)	1.932(5)	1.93(1)
C(6)–N(6)	1.161(7)	1.14(2)
Fe(1)–C(1)–N(1)	177.4(6)	178(1)
Fe(1)–C(2)–N(2)	177.4(5)	178(1)
Fe(1)–C(3)–N(3)	179.7(5)	178(1)
Fe(1)–C(4)–N(4)	177.9(5)	179(1)
Fe(1)–C(5)–N(5)	185.7(6)	177(1)
Fe(1)–C(6)–N(6)	177.5(5)	177(1)
Ln(1)–N(6)–C(6)	165.0(4)	164(1)

TABLE III Possible hydrogen bonding distances (Å)

D···*A*	**3**	**4**
O(8)···N(1)	2.801(8)	2.81(1)
O(8)···N(2)	2.883(7)	2.87(2)
O(8)···O(6)	2.672(5)	2.65(1)
N(4)···O(5)	2.829(7)	2.81(1)
N(4)···O(6)	2.862(7)	2.87(1)

165.0(4) and 164(1)° and the bond angles of Fe(1)–C(6)–N(6) are 177.5(5) and 177(1)° for **3** and **4**, respectively. The bonds on both sides of the cyanide bridge are large enough to weaken the magnetic interaction between Ln(III) and Fe(III) ions. The distances between the metal ions are Sm···Fe = 5.54 and Gd···Fe = 5.52 Å for **3** and **4**, respectively, indicating that there are no direct spin interactions between the 3d–4f ions [21].

Intermolecular hydrogen bonding and van der Waals cohesive forces are important in the formation of the crystals of **1**–**4**. Possible intermolecular and intramolecular bond distances are listed in Table III. The hydrogen bonds are suggested to be present in the case of O···N and/or O···O distances less than 3.2 Å, which is shorter than the sum of the van der Waals radii [17]. Consequently, three hydrogen bonds form among the crystalline water O(8), coordination water O(6), and cyanides N(1) and N(2). Another two hydrogen bonds form among the cyanides N(4) and the coordination water O(5) and O(6). Thus, a three-dimensional coordination polymer is formed through the intermolecular hydrogen bonds (Fig. 3). It is proposed that the network structure plays an important role in the antiferromagnetic interactions between the

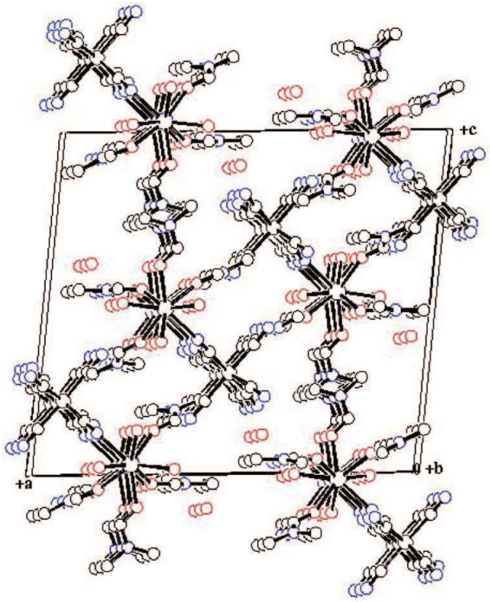

FIGURE 3 Crystal packing for **3** viewed down the crystallographic *c*-axis.

Ln(III) ions at a very low temperature, as has been observed in many 3d–4f bimetallic assemblies [7]. The cooperativity arising from the network through the intermolecular hydrogen bonds enhances the weak spin interaction between the Ln(III) ions, enabling it to be observed at lower temperature. However, no notable differences in terms of structure factors, corresponding to the differences with regard to magnetic properties, are observed between **3** and **4**. Therefore, the different magnetic properties among **1**–**4** may be attributed to the electronic states of Ln(III) ions based on structural considerations (discussed later).

Mössbauer Spectroscopy

Mössbauer spectra for **1**–**4** were recorded at both 298 and 10 K. The important parameters are listed in Table IV. A representative diagram is shown in Fig. 4. All of the spectra show that the quadrupole splitting remains at both 298 and 10 K, indicating typical low-spin Fe(III) ions ($S = 1/2$) like $K_3[Fe(CN)_6]$ and related compounds [18,19]. This reveals that the spin states of Fe(III) ions for **1**–**4** are not affected by temperature. However, slight changes in isomer shift, and relatively large changes in quadrupole splitting and line-width (half-width) for all compounds are observed with temperature. Nevertheless, no significant differences with respect to Mössbauer spectra, corresponding to the differences pertaining to magnetic properties, were observed among **1**–**4**. Therefore, the ground states of Ln(III) ions with odd $4f^n$ electrons ($n = 1$, 3, 5 and 7), $^2F_{5/2}$, $^4I_{9/2}$, $^6H_{5/2}$ and $^8S_{7/2}$ for anisotropic Ce(III), Nd(III), Sm(III) and isotropic Gd(III), dominate the exchange interaction in the Ln(III)–NC–Fe(III) systems, such as antiferromagnetic interaction for **1**, **2** and **4** and also a negligible interaction for **3** [7]. Recently, Yan and Chen determined that the magnetic coupling constant J was positive

TABLE IV Mössbauer parameters ($mm\,s^{-1}$) for **1**–**4**

Compound	*T* (K)	*IS*	*QS*	*HW*
1	297	−0.256	0.482	0.244
	10	−0.211	0.692	0.450
2	297	−0.276	0.499	0.260
	10	−0.237	0.717	0.521
3	297	−0.255	0.495	0.265
	10	−0.180	0.805	0.626
4	297	−0.231	0.484	0.267
	10	−0.184	0.781	0.594
$K_3[Fe(CN)_6]$ [18]	RT	−0.122	−0.288	0.242

IS, isomer shift; QS, quadrupole splitting; HW, half-width.

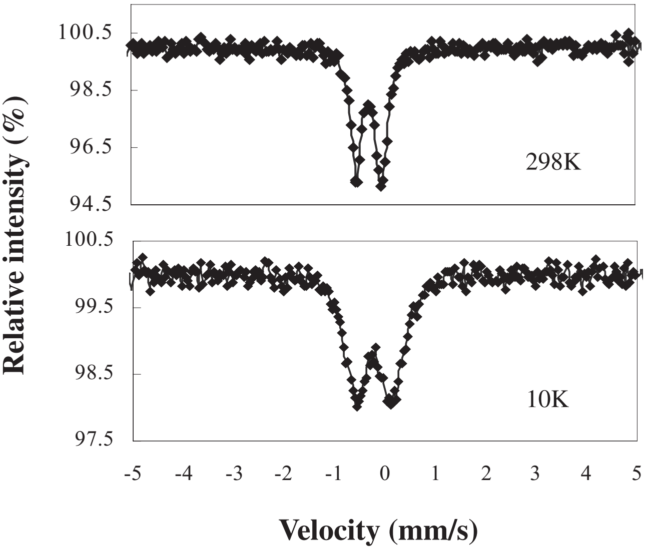

FIGURE 4 Representative Mössbauer spectra of **4** at 298 and 10 K.

(ferromagnetic) for $[Gd(C_4H_7ON)_4(H_2O)_3Fe(CN)_6]\cdot H_2O$ by means of density functional theory combined with the broken symmetry approach [3]. In the case of ladder-type Ln(III)–Cu(II) (^2D) systems, the overall interaction is antiferromagnetic for Ce(III) ($^2F_{5/2}$), Nd(III) ($^4I_{9/2}$) and Sm(III) ($^6H_{5/2}$) with nonzero total orbital angular momentum, whereas only the spin–spin interaction is ferromagnetic for Gd(III) ($^8S_{7/2}$) with zero orbital angular momentum [20]. Thus, not only the bridging geometries but also the magnetic anisotropy of the Ln(III) ions affect the magnetic properties of 3d–4f bimetallic assemblies [21,22].

CONCLUSION

Two new crystal structures, **3** and **4**, determined by X-ray crystallographic analysis are isomorphous to most of their analogs. However, **3** is different from the previously reported samarium compound in which the Sm atoms are nine-coordinate. Comparison of the important structural factors suggests that the significant differences in the magnetic properties between **3** and **4** do not derive from structural differences. Furthermore, Mössbauer spectra do not reveal any essential differences between **3** and **4** with regard to magnetic properties, which were collected for the first time for this series of compounds. The geometry of bridged-metal ions and the spin states of Fe(III) ions affect the type of exchange interaction in some cases. Therefore, this work supports the contention that magnetic anisotropy derived from the ground states of Ln(III) ions dominates exchange interactions of the Ln(III)–NC–Fe(III) systems.

Supplementary Material

Crystallographic data for the structural analysis have been deposited in the Cambridge Crystallographic Centre, CCDC Nos 204547 and 204548 for **3** and **4**, respectively. Copies of this information may be obtained free of charge from The Director, CCDC, 12 Union Road, Cambridge CB2 1EZ, UK (fax: +44-1233-336-033; e-mail: deposit@ccdc.cam.ac.uk or http://www.ccdc.cam.ac.uk).

Acknowledgments

This work was supported by Grant-in-Aid for Scientific Research on Priority Areas (417) and for the 21st century COE program "Keio Life Conjugate Chemistry" from the Ministry of Education, Culture, Sports, Science, and Technology (MEXT) of Japan.

References

[1] M. Katada, T. Nawa, H. Kumagai, S. Kawata and S. Kitagawa, *J. Radioanal. Nucl. Chem.* **2**, 227 (1999).
[2] B. Yan and Z. Chen, *Helv. Chim. Acta* **84**, 817 (2001).
[3] B. Yan and Z. Chen, *J. Phys. Chem.* **A104**, 6295 (2002).
[4] D. Mullica, J.M. Farmer, B.P. Cunningham and J.A. Kautz, *J. Coord. Chem.* **49**, 239 (2000).
[5] (a) J.A. Kautz, D.F. Mullica, B.P. Cunningham, R.A. Combs and J.M. Farmer, *J. Mol. Struct.* **523**, 175 (2000); (b) G. Li, T. Akitsu, O. Sato and Y. Einaga, *J. Am Chem. Soc.* **125**, 12396 (2003); G. Li, T. Akitsu, O. Sato and Y. Einaga, *J. Coord. Chem.* **57**, 189 (2004).
[6] H.-Z. Kou, G.-M. Yang, D.-Z. Liao, P. Cheng, Z.-H. Jiang, S.-P. Yan, X.-Y. Huang and G.-L. Wang, *J. Chem. Crystallogr.* **28**, 303 (1998).
[7] A. Figuerola, D. Camen, J. Ribas, V. Tangoulis, J. Granell, F. Lloret, J. Mahia and M. Maestro, *Inorg. Chem.* **42**, 641 (2003).
[8] T. Mallah, S. Tiebaut, M. Verdaguer and P. Veillet, *Science* **262**, 1554 (1993).
[9] teXsan, Crystal Structure Analysis Package (Molecular Structure Corporation, The Woodlands, TX, 1992 and 1995.
[10] A. Altomare, M.C. Burala, M. Cammalli, G. Cascarano, C. Giacocazzo, A. Guagliardi and G. Polidori, *J. Appl. Crystallogr.* **27**, 435 (1994).
[11] G.M. Sheldrick, SHELXL 97: Program for the Refinement of Crystal Structures (University of Göttingen, Germany, 1997).
[12] B.P. Cunningham and J.A. Kautz, *J. Chem. Crystallogr.* **30**, 671 (2000).
[13] E.N. Rizkalla and G.R. Choppin, In: K.A. Gschneidner, Jr. and L. Eyring (Eds.), Handbook on the Physics and Chemistry of Rare Earths (Elsevier, Amsterdam, 1995), Chapter 145, Vol. 21, pp. 305–366.
[14] R.D. Shannon, *Acta Crystallogr.* **A32**, 751 (1976).
[15] A. Bondi, *J. Phys. Chem.* **68**, 441 (1964).
[16] CSD, Cambridge Structural Database System, Cambridge Crystallographic Data Centre, University Chemical Laboratory, Cambridge, UK.

[17] G.R. Desiraju and T. Steiner, The Weak Hydrogen Bond (Oxford University Press, 1999).
[18] A. Vertes, L. Korecz and K. Burger, Mössbauer Spectroscopy (Elsevier, Amsterdam, 1979).
[19] (a) C.P. Monaghan and J.C. Fanning, *J. Phys. Chem.* **82**, 2 (1978); (b) E. Reguera and J.F. Bertran, *Hyperfine Interact.* **88**, 49 (1994); (c) K. Maer, Jr., M.L. Beasley, R.L. Collins and W.O. Milligan, *J. Am. Chem. Soc.* **90**, 3201 (1968).
[20] M.L. Kahn, C. Mathoniere and O. Kahn, *Inorg. Chem.* **38**, 3692 (1999).
[21] J.-P. Costes, F. Dahan, A. Dupuis and J.-P. Laurent, *Chem. Eur. J.* **4**, 1616 (1998).
[22] J.-C.G. Bunzli and C. Piguet, *Chem. Rev.* **102**, 1897 (2001).